International Journal of Applied Engineering Research ISSN 0973-4562 Volume 14, Number 21 (2019) pp. 4055-4066

Hall effects on MHD Oscillatory flow of Second grade fluid through Porous medium in a Parallel plate channel

P.M.Sadiq Basha[1*] and N. Nagarathna[2]

[1]*Department of Mathematics, Rayalaseema University, Kurnool, Andhra Pradesh - 518007, India.*

[2]*Department of Mathematics, Maharani's Science College for Women, Palace Road, Banglore – 560001, Karnataka, India.*

Abstract

In this paper, we have considered the unsteady two dimensional MHD oscillatory flow of blood in a porous arteriole under the influence of uniform transverse magnetic field in a parallel plate channel taking Hall current into account. Heat and mass transfer during arterial blood flow through porous medium are also studied. A mathematical model is developed for unsteady state situations using slip conditions. The unsteady hydromagnetic equations are solved by using regular perturbation method. Analytical expressions for the velocity, temperature and concentration profiles, wall shear stress and rates of heat and mass transfer have been obtained and computationally discussed with respect to the non-dimensional parameters. We concluded that the velocity reduces with increasing Hartmann number and enhances with Hall parameter and permeability parameter. Blood visco-elasticity lesser flow velocity significantly. The resultant velocity enhance with increasing thermal Grashof number, mass Grashof number and slip parameter. At any particular location as the thermal radiation increases, both heat transfer rate and temperature are reduced to an appreciable extent. However, the velocity is not significantly affected by thermal radiation.

Keywords: Heat transfer; mass transfer; chemical reaction; oscillatory flow; blood flow; hall current effect

1. INTRODUCTION

Paces of many physiological functions, including the flow through blood vessels are affected by drugs. The rates of different biochemical reactions that are responsible for the contraction muscles, secretion of different materials such as insulin, mucus and stomach acid by the glands and the transmission of massages by the nerves can be accelerated or decelerated by the action of drugs. The rate at which the kidney cells perform the regulation of the volume of water/salts in the body is affected by drugs. The rate at which blood flows through arteries can also be enhanced or slowed down by the application of drugs.

Hall effects on MHD flow through an accelerated plate in a rotating system in the presence of a magnetic field was examined by Deka [4]. Hydromagnetic channel flows in a rotating fluid system are investigated by researchers, Ghosh et al. [5]. Hydromagnetic convection flow in a rotating porous medium or in a channel partially filled by a porous medium with Hall effects are investigated by researchers such as Krishna et al. [6]. Chauhan and Agrawal [7-8], Dileep.D.C. [9] discussed the unsteady MHD flow of viscous incompressible and electrically conducting fluid through a porous medium adjacent to an accelerated impermeable plate in a rotating system taking Hall current into account, Heat transfer is also determined. Veera Krishna and Prakash [10] discussed the unsteady flow of an incompressible viscous fluid in a rotating parallel plate channel bounded on one side by a porous bed under the influence of a uniform transverse magnetic field taking hall current into account. Ashaf et al. [11] discussed Solution of MHD flow past a vertical porous plate through a porous medium under oscillatory suction. Lakshmanna and Venkateswarlu[12] discussed Heat and Mass Transfer on MHD Flow of an incompressible fluid past an infinite vertical porous plate. Krishna and Gangadhara Reddy [13] discussed the unsteady MHD free convection in a boundary layer flow of an electrically conducting fluid through porous medium subject to uniform transverse magnetic field over a moving infinite vertical plate in the presence of heat source and chemical reaction. Krishna and Subba Reddy [14] have investigated the simulation on the MHD forced convective flow through stumpy permeable porous medium (oil sands, sand) using Lattice Boltzmann method. Krishna and Jyothi [15] discussed the Hall effects on MHD Rotating flow of a visco-elastic fluid through a porous medium over an infinite oscillating porous plate with heat source and chemical reaction. B.S.K. Reddy et al.[16] investigated MHD flow of viscous incompressible nano-fluid through a saturating porous medium. Krishna et al. [17-20] discussed the MHD flows of an incompressible and electrically conducting fluid in planar channel. Veera Krishna et al. [21] discussed heat and mass transfer on unsteady MHD oscillatory flow of blood through porous arteriole. The effects of radiation and Hall current on an unsteady magnetohydrodynamic free convective flow in a vertical channel filled with a porous medium have been studied by Veera Krishna et al. [22]. Veera Krishna and Chamkha [23] investigated The diffusion-thermo, radiation-absorption and Hall and ion slip effects on MHD free convective rotating flow of nano-fluids (Ag and TiO2) past a semi-infinite permeable moving plate with constant heat source. Veera Krishna et al.[24] discussed the Soret and Joule effects of MHD mixed convective flow of an incompressible and electrically conducting viscous fluid past an infinite vertical porous plate taking Hall effects into account. Veera Krishna and Chamkha [25] discussed the MHD squeezing flow of a water-based nanofluid through a saturated porous medium between two parallel disks, taking the Hall current into account. Keeping the above mentioned facts, in this paper, we have considered the unsteady two dimensional MHD oscillatory flow of blood in a porous arteriole under the influence of uniform transverse magnetic field in a parallel plate channel taking Hall current into account.

2. FORMULATION AND SOLUTION OF THE PROBLEM

The circulatory system mainly consists of three-dimensional cylindrical vessels. However, in some cases, such as in micro vessels of the lungs, motion of blood can be approximately considered as channel flow. With this consideration, as in many other similar theoretical studies (e.g. [2]), the formulation analysis that follows, we use Cartesian coordinates. The flow is considered symmetric about the axis of the channel and driven by the stretching of the channel wall, such that the velocity of each wall is proportional to the axial coordinate. In order to study the second-order effects of unsteady MHD flow of blood taking Hall current into account, let us first consider the flow of a second-order fluid between two parallel plates at z=0 and z=h, where the x-axis is taken parallel length of plates and z-axis along a direction perpendicular to the plates.

The model developed here pertains to a pathological state of an arterial segment (as in the case of multiple atherosclerosis), when the lumen has turned porous due to the deposition of different materials such as cholesterol, lipids and fatty substances. The physical sketch of the problem is similar to that in [1, 2]. Taking into account the existence of slip between the velocity of blood and the arterial wall tissues, the relative velocity between blood and the arterial wall is assumed to be proportional to the shear rate at the wall. Blood is considered as a suspension of erythrocytes and other micro-elements in plasma. It is assumed that in the segment under consideration, blood is uniformly dense. A magnetic field of constant intensity

B_0 is considered to be applied in the *y*-direction.

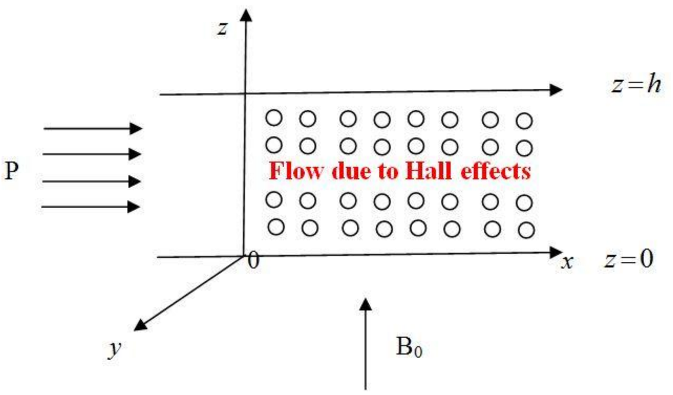

Fig. 1 Physical configuration of the Problem

The unsteady hydromagnetic equations of the momentum, heat transfer and mass transfer for the MHD oscillatory flow of second grade fluid through a porous arteriole in the parallel plate system are considered in the form (Makinde and Mhone [3]).

$$\frac{\partial w}{\partial z} = 0 \tag{1}$$

$$\frac{\partial u}{\partial t} = -\frac{1}{\rho}\frac{\partial p}{\partial x} + \nu\frac{\partial^2 u}{\partial z^2} + \frac{\alpha_1}{\rho}\frac{\partial^3 u}{\partial z^2 \partial t} + B_0 J_y - \frac{\nu}{k}u + g\beta(T - T_\infty) + g\beta^*(C - C_\infty) \tag{2}$$

$$\frac{\partial v}{\partial t} = -\frac{1}{\rho}\frac{\partial p}{\partial y} + \nu\frac{\partial^2 v}{\partial z^2} + \frac{\alpha_1}{\rho}\frac{\partial^3 v}{\partial z^2 \partial t} - B_0 J_x - \frac{\nu}{k}v \tag{3}$$

$$\frac{\partial T}{\partial t} = \frac{K_1}{\rho C_p}\frac{\partial^2 T}{\partial z^2} - \frac{1}{\rho C_p}\frac{\partial q_r}{\partial z} \tag{4}$$

$$\frac{\partial C}{\partial t} = D\frac{\partial^2 C}{\partial z^2} - K_c(C - C_0) \tag{5}$$

Where, the meanings of all the symbols appearing in the equations have their usual meaning. When the strength of the magnetic field is very large, the generalized Ohm's law is modified to include the hall current so that

$$J + \frac{\omega_e \tau_e}{B_O}(J \times B) = \sigma\left[E + V \times B + \frac{1}{e\eta_e}\nabla P_e\right] \tag{6}$$

Where ω_e is the cyclotron frequency of the electrons, τ_e is the electron collision time, σ is the electrical conductivity, e is the electron charge and P_e is the electron pressure. The ion-slip and thermo electric effects are not included in equation (6). Further, it is assumed that $\omega_e \tau_e$ ~ O(1) and $\omega_i \tau_i << 1$, where ω_i and τ_i are the cyclotron frequency and collision time for ions respectively. In equation (6) the electron pressure gradient, the ion-slip and thermoelectric effects are neglected. We also assume that the electric field *E=0* under assumptions reduces to

$$J_x + m\, J_y = \sigma B_0 v \tag{7}$$

$$J_y - m\, J_x = -\sigma B_0 u \tag{8}$$

Where, $m = \tau_e \omega_e$ is the hall parameter.

On solving equations (7) and (8) we obtain

$$J_x = \frac{\sigma B_0}{1+m^2}(v+mu) \quad (9)$$

$$J_y = \frac{\sigma B_0}{1+m^2}(mv-u) \quad (10)$$

Substituting the equations (9) and (10) in (3) and (2) respectively, we obtain

$$\frac{\partial u}{\partial t} = -\frac{1}{\rho}\frac{\partial p}{\partial x} + \nu\frac{\partial^2 u}{\partial z^2} + \frac{\alpha_1}{\rho}\frac{\partial^3 u}{\partial z^2 \partial t} - \left(\frac{\sigma B_0^2}{\rho(1+m^2)} + \frac{\nu}{k}\right)u + g\beta(T-T_\infty) + g\beta^*(C-C_\infty) \quad (11)$$

$$\frac{\partial v}{\partial t} = -\frac{1}{\rho}\frac{\partial p}{\partial y} + \nu\frac{\partial^2 v}{\partial z^2} + \frac{\alpha_1}{\rho}\frac{\partial^3 v}{\partial z^2 \partial t} - \left(\frac{\sigma B_0^2}{\rho(1+m^2)} + \frac{\nu}{k}\right)v \quad (12)$$

In presence of red cell-slip at the boundary wall of the blood vessels reported by Brunn [35] and Nubar [36].

The corresponding boundary conditions are

$$u = \lambda\frac{\partial u}{\partial z}, v = \lambda\frac{\partial v}{\partial z}, T = T_0 + (T_w - T_0)e^{i\omega t}, \quad C = C_0 + (C_w - C_0)e^{i\omega t} \quad \text{at} \quad z = h \quad (13)$$

$$u = \lambda\frac{\partial u}{\partial z}, v = \lambda\frac{\partial u}{\partial z}, T = T_0, C = C_0 \quad \text{at} \quad z = 0 \quad (14)$$

Using Rosseland approximation [37], the radiative transfer term q_r in Eq. (4) may be expressed as

$$q_r = -\frac{4\sigma^*}{3\alpha_r}\frac{\partial T^4}{\partial z} \quad (15)$$

We assume that the temperature differences within the flow are such that T^4 can be expressed as a linear function of the temperature *T*. This is accomplished by expanding T^4 in a Taylor series about T_0 (which is assumed to be independent of *z*) and neglecting powers of *T* higher than the first. Thus we have

$$T^4 = 4T_0^3 T - 3T_0^4 \quad (16)$$

Then the heat transfer equation becomes

$$\frac{\partial T}{\partial t} = \frac{K_1}{\rho C_p}\frac{\partial^2 T}{\partial z^2} - \frac{16\sigma^* T_0^3}{3\rho C_p \alpha_r}\frac{\partial^2 T}{\partial z^2} \quad (17)$$

Combining the equations (11) and (12), $q = u + iv,\ \xi = x - iy$ and we obtain

$$\frac{\partial q}{\partial t} = -\frac{1}{\rho}\frac{\partial p}{\partial \xi} + \nu\frac{\partial^2 q}{\partial z^2} + \frac{\alpha_1}{\rho}\frac{\partial^3 q}{\partial z^2 \partial t} - \left(\frac{\sigma B_0^2}{\rho} + \frac{\nu}{k}\right)q + g\beta(T-T_\infty) + g\beta^*(C-C_\infty) \quad (18)$$

We now introduce the following non-dimensional variables:

$$x^* = \frac{x}{h}, y^* = \frac{y}{h}, z^* = \frac{z}{h}, q^* = \frac{q}{U_0}, t^* = \frac{tU_0}{h}, \theta = \frac{T-T_0}{T_w - T_0},$$

$$\phi = \frac{C-C_0}{C_w - C_0}, \omega^* = \frac{\omega h}{U_0}, t^* = \frac{tw_0^2}{\nu}, \xi^* = \frac{\xi}{h}, p^* = \frac{p}{\rho U_0^2}$$

Making use of non-dimensional quantities (dropping asterisks), the governing equation (18), (3) and (4) can be written as

$$\mathrm{Re}\frac{\partial q}{\partial t} = -\frac{\partial p}{\partial \xi} + \frac{\partial^2 q}{\partial z^2} + \alpha\frac{\partial^3 q}{\partial z^2 \partial t} - \left(\frac{M^2}{1+m^2} + \frac{1}{K}\right)q + \mathrm{Gr}\,\theta + \mathrm{Gc}\,\phi \quad (19)$$

$$\mathrm{Pr}\frac{\partial \theta}{\partial t} = (1+R)\frac{\partial^2 \theta}{\partial z^2} \quad (20)$$

$$\mathrm{Sc}\frac{\partial \phi}{\partial t} = \frac{\partial^2 \phi}{\partial z^2} - \mathrm{Kc}\,\phi \quad (21)$$

The corresponding non-dimensional boundary conditions assume the form

$$q = \lambda\frac{\partial q}{\partial z},\ \theta = e^{i\omega t}, \phi = e^{i\omega t} \quad \text{at} \quad z = 1 \quad (22)$$

$$q = \lambda\frac{\partial q}{\partial z},\ \theta = 0,\ \phi = 0 \quad \text{at} \quad z = 0 \quad (23)$$

Where,

$M^2 = \frac{\sigma B_0^2 h^2}{\rho\nu}$ is the Hartmann number (Magnetic field parameter), $K = \frac{k}{h^2\rho}$ is the Permeability parameter, $\alpha = \frac{\alpha_1 U_0}{\nu h}$ is the second grade fluid parameter,

$\mathrm{Gr}=\dfrac{g\beta(T_w-T_0)h^2}{\nu U_0}$ is the thermal Grashof number, $\mathrm{Gr}=\dfrac{g\beta^*(C_w-C_0)h^2}{\nu U_0}$ is the mass Grashof number, $\mathrm{Pr}=\dfrac{\rho C_p}{K_1}$ is Prandtl parameter, $R=\dfrac{16\sigma^* T_0^3}{3\alpha_r K_1}$ is the Radiation parameter, $\mathrm{Kc}=DK_c(C_w-C_0)$ chemical reaction parameter and $\mathrm{Sc}=\dfrac{\nu}{D}$ is the Schmidt number.

From Eq. (19), it follows that, $\partial p/\partial\xi$ is a function of *t* only. We consider it to be of the form,

$$\frac{\partial p}{\partial \xi}=Pe^{i\omega t} \tag{24}$$

To solve Eqs. (19), (20) and (21) subject to the boundary conditions (22) and (23), we further write the velocity, temperature and concentration as

$$q(z,t)=q_1e^{i\omega t} \tag{25}$$

$$\theta(z,t)=\theta_1e^{i\omega t} \tag{26}$$

$$\phi(z,t)=\phi_1e^{i\omega t} \tag{27}$$

Substituting these expressions (25), (26) and (27) in (19), (20) and (21) respectively and comparing the co-efficient of like terms we have the equations.

$$(1+\alpha i\omega)\frac{\partial^2 q_1}{\partial z^2}-\left(\mathrm{Re}i\omega+\frac{M^2}{1+m^2}+\frac{1}{K}\right)q_1 = -P-\mathrm{Gr}\,\theta_1-\mathrm{Gc}\,\phi_1 \tag{28}$$

$$(1+R)\frac{\partial^2\theta_1}{\partial z^2}-\mathrm{Pr}i\omega\theta_1=0 \tag{29}$$

$$\frac{\partial^2\phi_1}{\partial z^2}-(\mathrm{Sc}i\omega+\mathrm{Kc})\phi_1=0 \tag{30}$$

With corresponding boundary conditions

$$q=\lambda\frac{\partial q_1}{\partial z},\ \theta_1=1,\ \phi_1=1 \quad \text{at} \quad z=1 \tag{31}$$

$$q=\lambda\frac{\partial q_1}{\partial z},\ \theta_1=0,\ \phi_1=0 \quad \text{at} \quad z=0 \tag{32}$$

Solving (28) – (30) subject to the conditions (31) and (32), we have velocity field, temperature, concentration respectively, where the expressions for the constants $m_i(i=1,2,.....,6)$ and $a_i(i=1,2,.....,6)$ are given in Appendix.

$$q(z,t)=\left(a_1e^{m_1z}+a_2e^{m_2z}-\frac{P}{\mathrm{Re}i\omega+\frac{M^2}{1+m^2}+(1/K)}-\frac{\mathrm{Gr}}{e^{m_3}-e^{m_4}}\left[\frac{e^{m_3z}}{a_3}-\frac{e^{m_4z}}{a_4}\right]-\frac{\mathrm{Gc}}{e^{m_5}-e^{m_6}}\left[\frac{e^{m_5z}}{a_5}-\frac{e^{m_6z}}{a_6}\right]\right)e^{i\omega t} \tag{33}$$

$$\theta(z,t)=\frac{1}{e^{m_3}-e^{m_4}}\left(e^{m_3z}-e^{m_4z}\right)e^{i\omega t} \tag{34}$$

$$\phi(z,t)=\frac{1}{e^{m_5}-e^{m_6}}\left(e^{m_5z}-e^{m_6z}\right)e^{i\omega t} \tag{35}$$

The wall shear stress at the wall of the upper plate representing the upper wall of the blood vessel is found as

$$\tau_w=\left[\frac{\partial q}{\partial z}+\alpha\frac{\partial^2 q}{\partial z\partial t}\right]_{z=1} =\left(a_1m_1e^{m_1}+a_2m_2e^{m_2}-\frac{\mathrm{Gr}}{e^{m_3}-e^{m_4}}\left[\frac{m_3e^{m_3}}{a_3}-\frac{m_4e^{m_4}}{a_4}\right]-\frac{\mathrm{Gc}}{e^{m_5}-e^{m_6}}\left[\frac{m_5e^{m_5}}{a_5}-\frac{m_6e^{m_6}}{a_6}\right]\right)(1+\alpha i\omega)e^{i\omega t} \tag{36}$$

The rates of heat and mass transfer across the upper plate (upper wall) are calculated as

$$Nu=\left[-\frac{\partial\theta}{\partial z}\right]_{z=1}=-\frac{1}{e^{m_3}-e^{m_4}}\left(m_3e^{m_3}-m_4e^{m_4}\right)e^{i\omega t} \tag{37}$$

$$Sh=\left[-\frac{\partial\phi}{\partial z}\right]_{z=1}=-\frac{1}{e^{m_5}-e^{m_6}}\left(m_5e^{m_5}-m_6e^{m_6}\right)e^{i\omega t} \tag{38}$$

3. RESULTS AND DISCUSSION

All the computational data have been presented in graphical/tabular form. The flow governed by the non-dimensional parameters M Hartmann number, K permeability parameter, *m* the Hall parameter, Re the Reynolds number, α visco-elastic parameter, R radiation parameter, Gr thermal Grashof number, Gc mass Grashof number, Sc Schmidt number, ω the frequency of oscillation, λ slip velocity parameter, Kc the chemical reaction parameter. The velocity, temperature, concentration, the shear stresses at the boundaries, Nusselt number (Nu) and shearwood number (Sh) between the plates are evaluated analytically using regular perturbation technique and computationally discussed for different variations in the governing parameters. The Figs. 2-13 represent the velocity profiles for *u* and *v*; the Figs 14 represent the temperature profiles for θ; the Figs. 15 represent the concentration profiles for ϕ.

From the Figs. 2, we noticed that, both the velocity components *u* and *v* reduces with increasing the intensity of the magnetic field or Hartmann number *M*. Also we have been seen that the resultant velocity is experiences retardation throughout the fluid region. The velocity component *u* increases and *v* reduces with increasing permeability parameter *K* or Hall parameter *m*. The resultant velocity enhances with increasing *K* or *m* in the flow field. We also noticed that lower the permeability lesser the fluid speed is observed the entire fluid region (Figs. 3 & 7). The similar behaviour is observed for the velocity components with radiation parameter R (Fig. 9). This gives an idea of the influence of chemical reaction on the velocity distribution under identical condition of heat radiation. The magnitude of the velocity components *u* and *v* as well as resultant velocity reduces in the entire fluid region with increasing second grade fluid parameter α, Pr, Sc and Kc (Figs. 4, 5, 10 & 13). Also it indicates that at a particular instant of time, blood velocity reduces as blood visco-elasticity (α) increases. From the Figs (6 & 8), the velocity components *u* and *v* as well as resultant velocity increase with increasing thermal Grashof number Gr, mass Grashof number Gc. The similar behaviour is observed for λ, there is no indication of flow separation in the absence of slip velocity at the wall, but flow separation does take place whenever there is velocity-slip at the boundary. It is important to note that the extent of flow separation increases with the increase in the slip velocity parameter λ. We also find that the magnitude of the velocity component *u* reduces and *v* enhances with increasing the frequency of oscillation ω. The resultant velocity reduces throughout the fluid region with increasing the frequency of oscillation (Figs 12).

We noticed that from the Fig. (14), the magnitude of the temperature reduces with increasing radiation parameter R, where as the reversal behaviour is observed throughout the fluid region with increasing Prandtl number Pr. Also we found that from the Fig. (15), the magnitude of the concentration increases with increasing Schmidt number Sc, where as the reversal behaviour is observed throughout the fluid region with increasing chemical reaction parameter Kc. Finally, these reveal that under the purview of the present computational study, at any given distance the temperature/ concentration reduces as the thermal radiation/chemical reaction parameter increases. Further it reveals that for any particular values of thermal radiation/chemical reaction parameter, both the temperature and the concentration increase as we move further and further from the lower wall to the upper one.

The frictional force is determined at the upper wall are presented in the Table. 1. This shows that in the absence of any magnetic field, the wall shear stress increases with increase in the value of the Reynolds number, and there occurs a sharp reduction in the wall shear stress, which changes its nature from tensile to compressive. A similar nature of the shear stress is observed, even in the presence of a magnetic field of unit strength; however the change from tensile to compressive is somewhat smooth. The magnitude of the stress components τ_x and τ_y enhances with increasing K, Gr, Gc, *m* and λ. The opposite nature is observed for the same components with increasing *M* and Kc. The magnitude of the stress component τ_x reduces and τ_y increases with increasing α, ω and R. The reversal behaviour is for the components τ_x and τ_y with increasing Pr and Sc (Table 1).

We also noticed that from the table (2) the Nusselt number Nu enhances with increasing Radiation parameter R and Prandtl number Pr. Likewise the rate of mass transfer is reduces with increasing Schmidt number Sc and increases with increasing chemical reaction parameter Kc (Table 3).

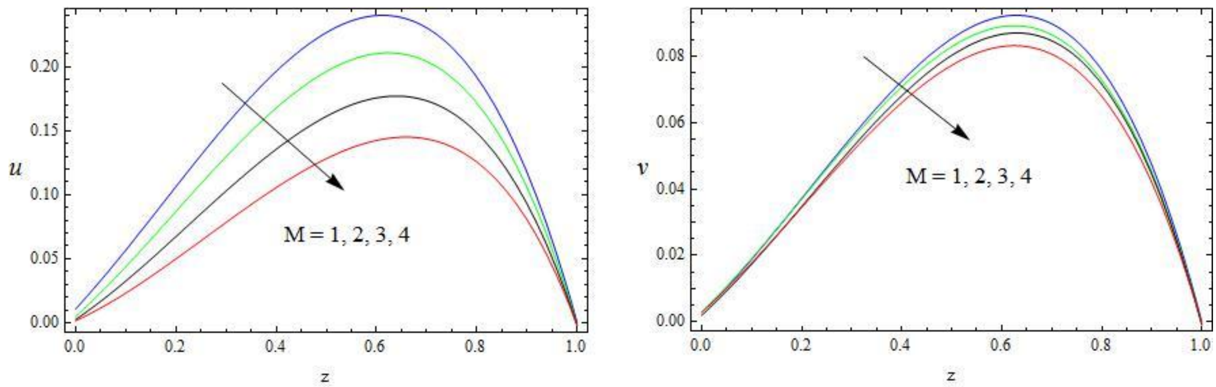

Fig. 2. The velocity Profiles for *u* and *v* against M with *t* = 1, Re=1

$$\mathrm{K} = 1, \alpha = 0.5, \mathrm{Pr} = 0.71, \mathrm{Gr} = 2, \mathrm{Gc} = 5, R = 0.5, \mathrm{Sc} = 0.22, \omega = \pi/4, \lambda = 0.002, \mathrm{Kc} = 0.5, m = 1$$

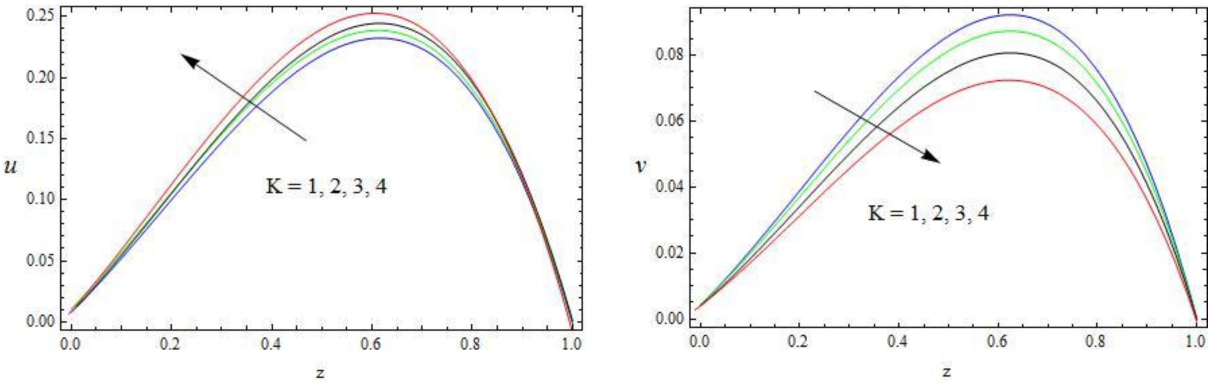

Fig. 3. The velocity Profiles for *u* and *v* against K with *t* = 1, Re=1

$M = 1, \alpha = 0.5, Pr = 0.71, Gr = 2, Gc = 5, R = 0.5, Sc = 0.22, \omega = \pi / 4, \lambda = 0.002, Kc = 0.5, m = 1$

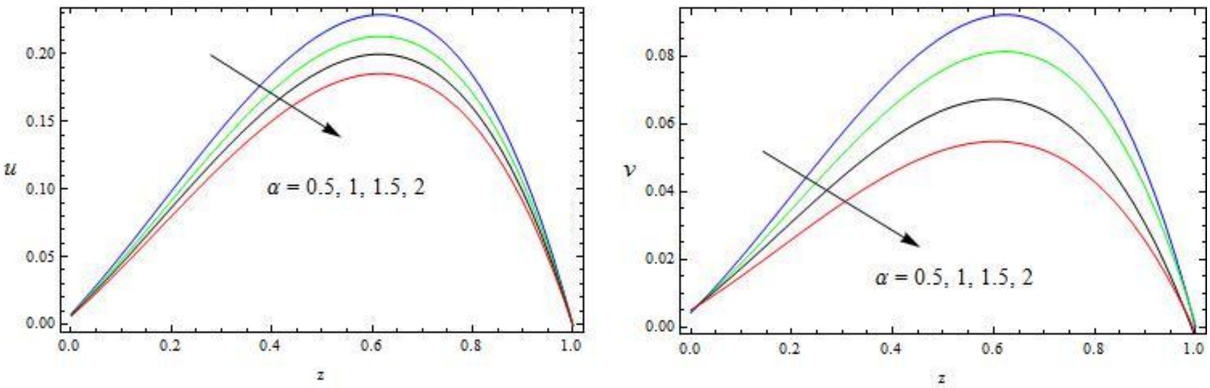

Fig. 4. The velocity Profiles for *u* and *v* against α with *t* = 1, Re=1

$K = 1, M = 1, Pr = 0.71, Gr = 2, Gc = 5, R = 0.5, Sc = 0.22, \omega = \pi / 4, \lambda = 0.002, Kc = 0.5, m = 1$

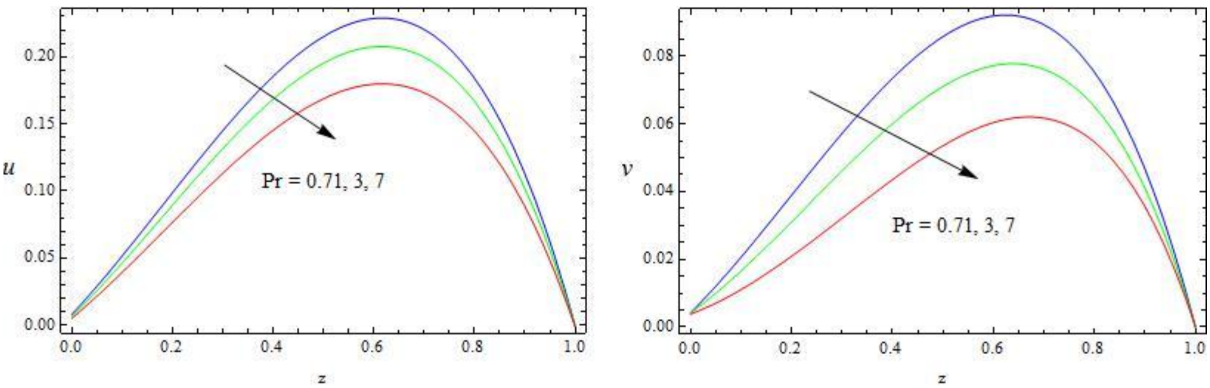

Fig. 5. The velocity Profile for *u* and *v* against Pr with *t* = 1, Re=1

$K = 1, \alpha = 0.5, M = 1, Gr = 2, Gc = 5, R = 0.5, Sc = 0.22, \omega = \pi / 4, \lambda = 0.002, Kc = 0.5, m = 1$

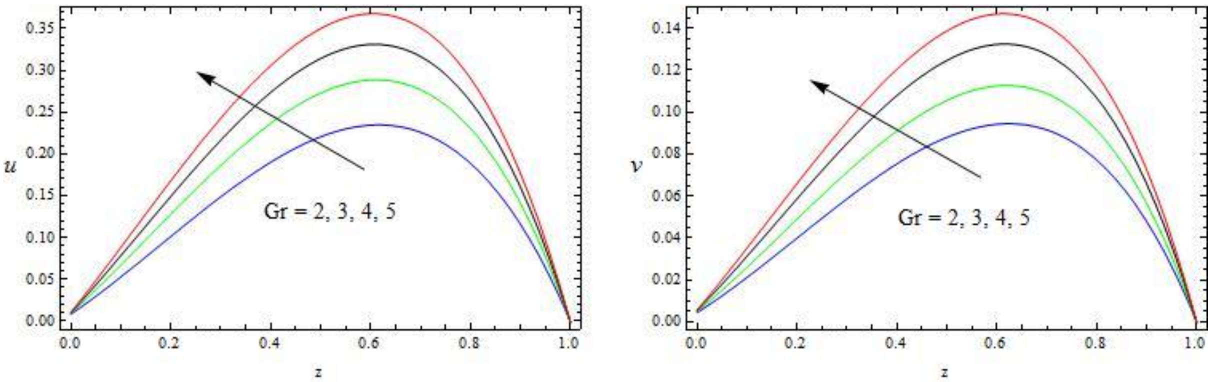

Fig. 6. The velocity Profiles for *u* and *v* against Gr with t = 1, Re=1

$$\mathrm{K}=1,\alpha=0.5,\mathrm{Pr}=0.71,\mathrm{M}=1,\mathrm{Gc}=5,R=0.5,\mathrm{Sc}=0.22,\omega=\pi/4,\lambda=0.002,\mathrm{Kc}=0.5,m=1$$

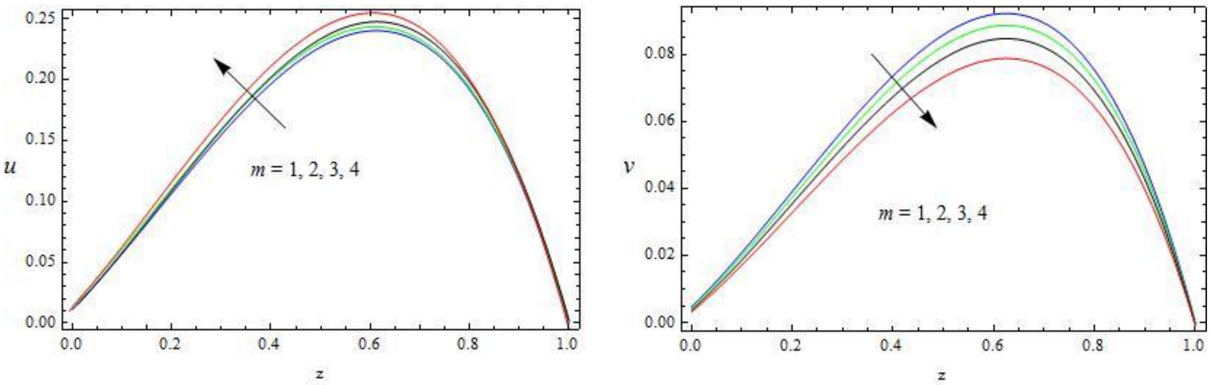

Fig. 7. The velocity Profiles for *u* and *v* against *m* with t = 1, Re=1

$$\mathrm{K}=1,\alpha=0.5,\mathrm{Pr}=0.71,\mathrm{M}=1,\mathrm{Gc}=5,R=0.5,\mathrm{Sc}=0.22,\omega=\pi/4,\lambda=0.002,\mathrm{Kc}=0.5,\mathrm{Gr}=2$$

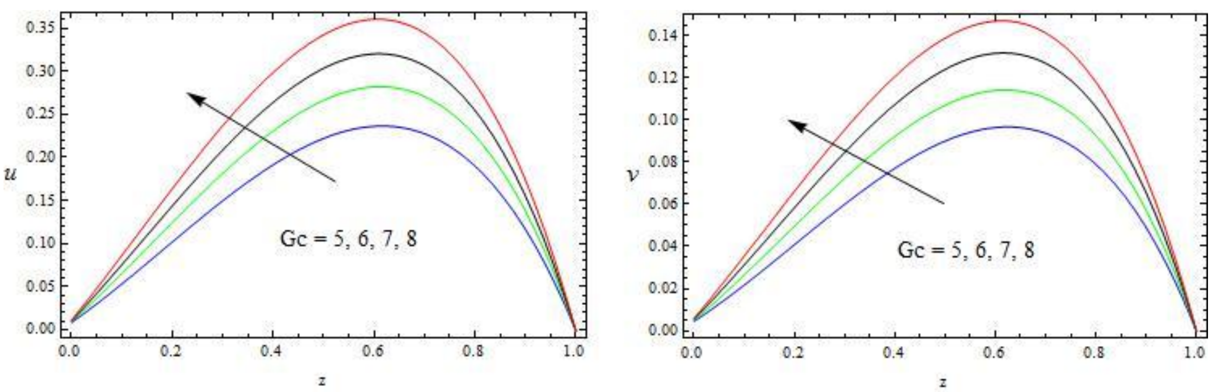

Fig. 8. The velocity Profiles for *u* and *v* against Gc with t = 1, Re=1

$$\mathrm{K}=1,\alpha=0.5,\mathrm{Pr}=0.71,\mathrm{Gr}=2,\mathrm{M}=1,R=0.5,\mathrm{Sc}=0.22,\omega=\pi/4,\lambda=0.002,\mathrm{Kc}=0.5,m=1$$

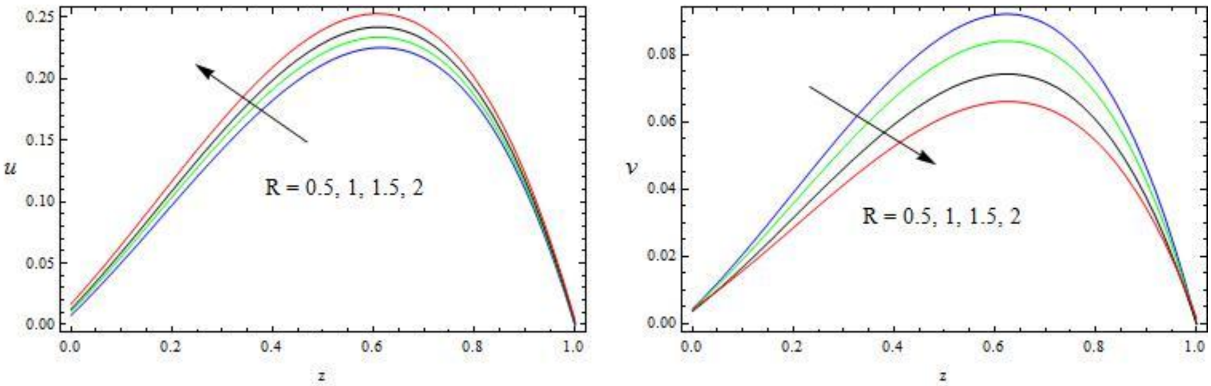

Fig. 9. The velocity Profiles for *u* and *v* against R with *t* = 1, Re=1

$\mathrm{K}=1, \alpha=0.5, \mathrm{Pr}=0.71, \mathrm{Gr}=2, \mathrm{Gc}=5, \mathrm{M}=1, \mathrm{Sc}=0.22, \omega=\pi/4, \lambda=0.002, \mathrm{Kc}=0.5, m=1$

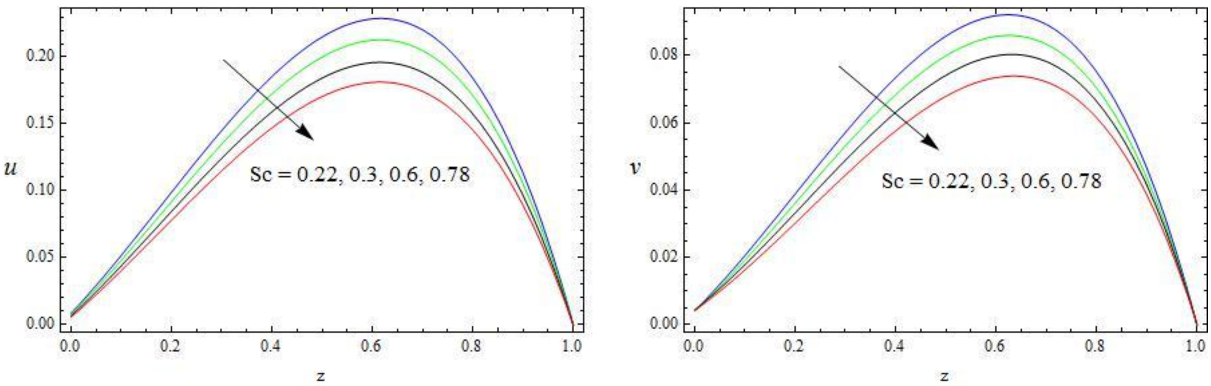

Fig. 10. The velocity Profiles for *u* and *v* against Sc with *t* = 1, Re=1

$\mathrm{K}=1, \alpha=0.5, \mathrm{Pr}=0.71, \mathrm{Gr}=2, \mathrm{Gc}=5, R=0.5, \mathrm{M}=1, \omega=\pi/4, \lambda=0.002, \mathrm{Kc}=0.5, m=1$

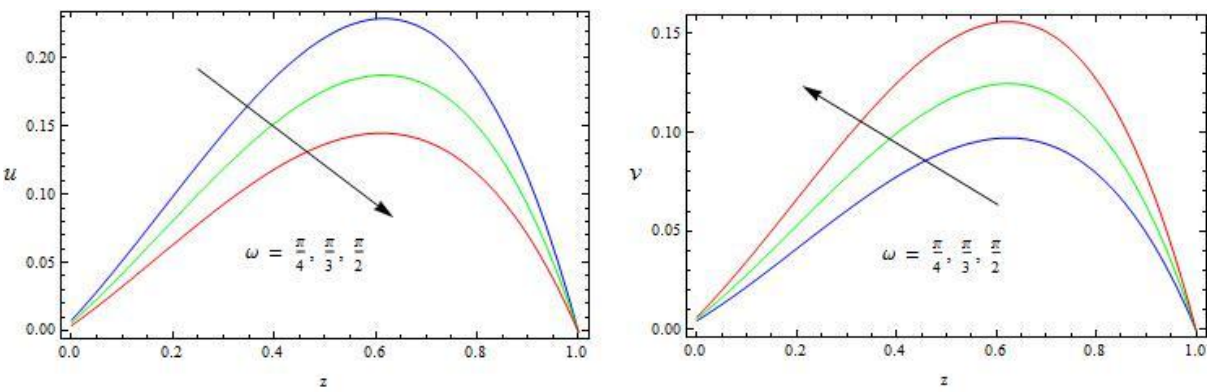

Fig. 11. The velocity Profiles for *u* and *v* against ω with *t* = 1, Re=1

$\mathrm{K}=1, \alpha=0.5, \mathrm{Pr}=0.71, \mathrm{Gr}=2, \mathrm{Gc}=5, R=0.5, \mathrm{Sc}=0.22, \mathrm{M}=1, \lambda=0.002, \mathrm{Kc}=0.5, m=1$

International Journal of Applied Engineering Research ISSN 0973-4562 Volume 14, Number 21 (2019) pp. 4055-4066

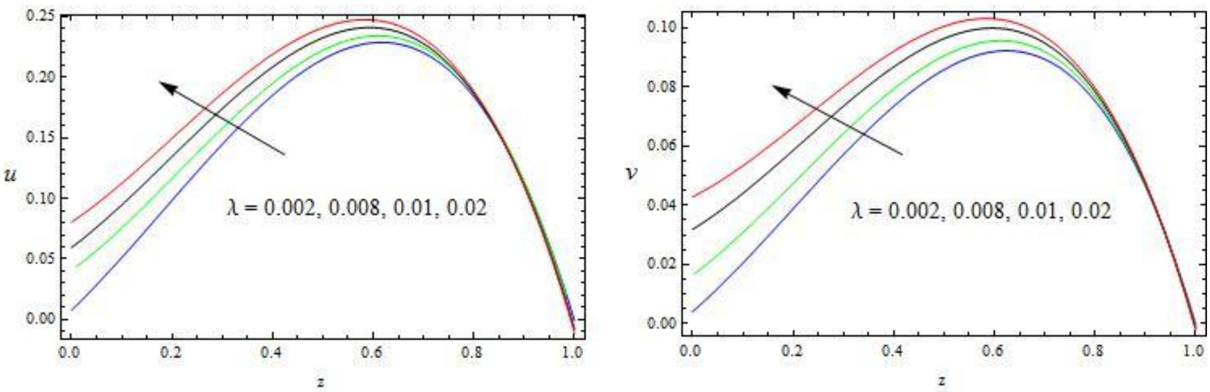

Fig. 12. The velocity Profiles for *u* and *v* against λ with *t* = 1, Re=1

$\mathrm{K} = 1, \alpha = 0.5, \mathrm{Pr} = 0.71, \mathrm{Gr} = 2, \mathrm{Gc} = 5, R = 0.5, \mathrm{Sc} = 0.22, \omega = \pi / 4, \mathrm{M} = 1, \mathrm{Kc} = 0.5, m = 1$

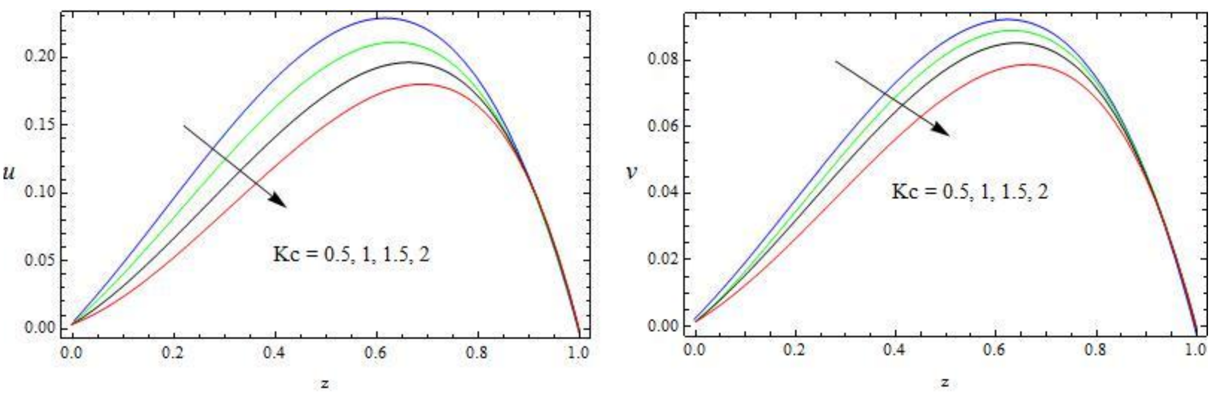

Fig. 13. The velocity Profiles for *u* and *v* against Kc with *t* = 1, Re=1

$\mathrm{K} = 1, \alpha = 0.5, \mathrm{Pr} = 0.71, \mathrm{Gr} = 2, \mathrm{Gc} = 5, R = 0.5, \mathrm{Sc} = 0.22, \omega = \pi / 4, \lambda = 0.002, \mathrm{M} = 1, m = 1$

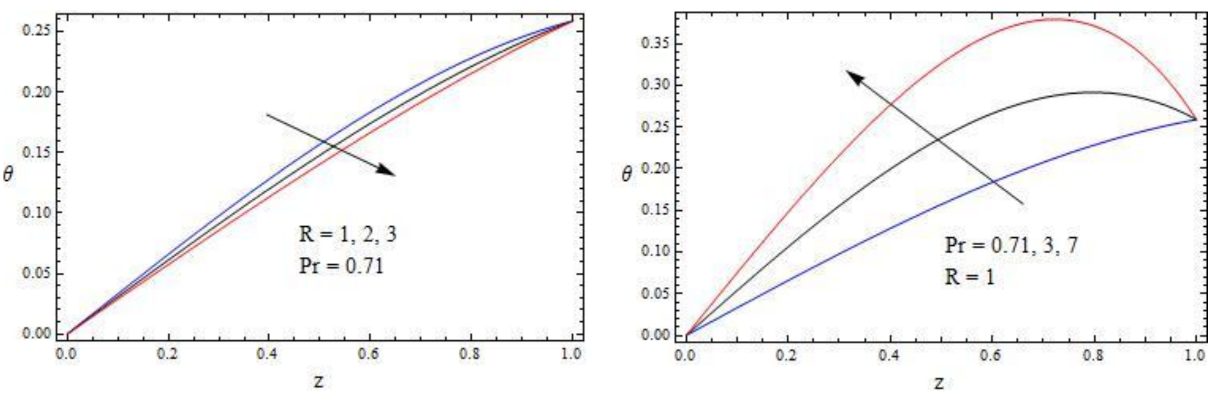

Fig. 14. The temperature Profiles for θ against R and Pr with $\omega = 5\pi / 12, \mathrm{t} = 0.1$

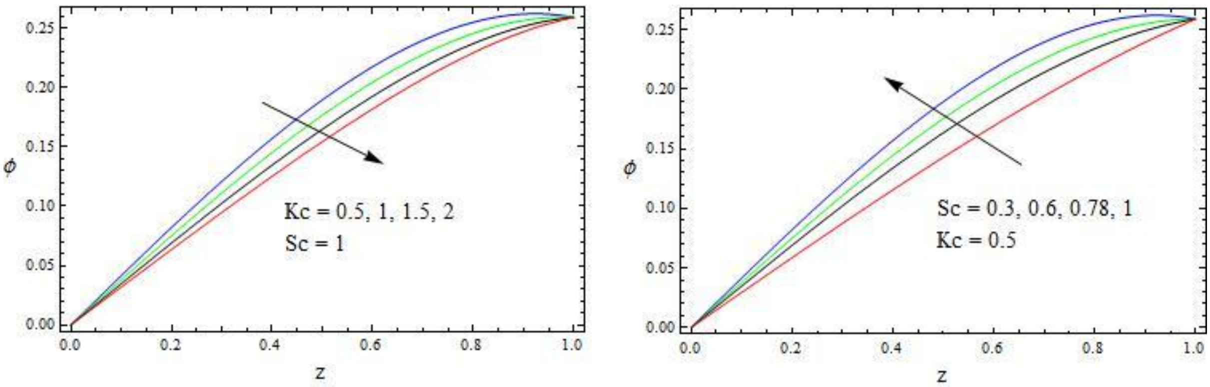

Fig. 15. The concentration Profiles for ϕ against Kc and Sc with $\omega = 5\pi/12, \mathrm{t} = 0.1$

Table 1. Skin Friction

M	K	α	R	Pr	Gr	Gc	Sc	ω	λ	Kc	*m*	$-\tau_x$	$-\tau_y$
1	**1**	**0.5**	**0.5**	**0.71**	**2**	**5**	**0.3**	$\pi/4$	0.002	**0.5**	**1**	1.194155	1.124449
2												1.095123	1.083292
3												0.972012	1.019974
	2											1.234540	1.138433
	3											1.249641	1.142705
		0.8										1.185716	1.150637
		1										1.184588	1.166308
			1									1.191836	1.127161
			1.5									1.190420	1.128767
				3								1.219310	1.086195
				7								1.240968	1.013843
					3							1.416274	1.332370
					4							1.638393	1.540291
						6						1.407755	1.328302
						7						1.621355	1.532154
							0.6					1.207231	1.108872
							0.78					1.214729	1.099162
								$\pi/3$				0.872493	1.384037
								$\pi/2$				0.088971	1.624961
									0.008			1.215191	1.145498
									0.01			1.222270	1.152589
										1.0		1.163961	1.097990
										1.5		1.133286	1.088130
											2	1.217668	1.132895
											3	1.225958	1.135689

Table 2: Nusselt number

R	Pr	ω	Nu
0.5	**0.71**	$5\pi/12$	−0.062010
1			−0.110643
1.5			−0.140021
2			−0.159684
	3		0.512785
	7		1.209667

Table 3: Sherwood number

Sc	Kc	ω	Sh
0.3	**0.5**	$5\pi/12$	−0.182881
0.6			−0.067315
0.78			0.000764
1			0.082496
	1		−0.228894
	1.5		−0.271903

Table 4: Comparison of Results for resultant velocity (q)

$\mathrm{Gr}=2, \mathrm{Gc}=5, \mathrm{Sc}=0.3, \omega=\pi/4, z=0.2$

M	***K***	α	**R**	Previous Results Krishna et al.[21] $m=0$	Present Results
1	**1**	**0.5**	**0.5**	0.142551	0.142557
2				0.135524	0.135529
3				0.120554	0.120558
	2			0.166589	0.166594
	3			0.185547	0.185552
		0.8		0.128579	0.128586
		1		0.102455	0.102461
			1	0.157748	0.157756
			1.5	0.166087	0.166093

4. CONCLUSIONS

We have considered the unsteady two dimensional MHD oscillatory flow of second grade fluid in a porous medium under the influence of uniform transverse magnetic field in a parallel plate channel taking Hall current into account. The study enables us to conclude the following:

1. The velocity reduces with increasing Hartmann number *M* and enhances with permeability parameter *K* or Hall parameter *m*.
2. Blood visco-elasticity lesser flow velocity significantly.
3. The resultant velocity enhance with increasing thermal Grashof number, mass Grashof number and slip parameter
4. The wall shear stress is strongly pretentious by the Reynolds number.
5. At any particular location as the thermal radiation increases, both heat transfer rate and temperature are reduced to an appreciable extent. However, the velocity is not significantly affected by thermal radiation.
6. The rate of Heat transfer boosts with increasing Prandtl number.
7. Concentration and rate of mass transfer are abridged due to chemical reaction. Comparatively, the velocity distribution is less affected due to chemical reaction.
8. The rate of mass transfer is enhanced, as the mass diffusivity reduces (i.e. as the Schmidt number increases).

REFERENCES

[1]. A. Sinha, J.C. Misra, MHD flow of blood through a dually stenosed artery: effects of viscosity variation, variable hematocrit and velocity-slip, Can. J. Chem. Eng. 92 (2014) 23–31.

[2]. J.C. Misra, A. Sinha, G.C. Shit, Flow of a biomagnetic viscoelastic fluid: application to estimation of blood flow in arteries during electromagnetic hyperthermia, a therapeutic procedure for cancer treatment, Appl. Math. Mach. 31 (2010) 1405–1420.

[3]. O.D. Makinde, P.Y. Mhone, Heat transfer to MHD oscillatory flow in a channel filled with porous medium, Rom. J. Phys. 50 (2005) 931–938.

[4]. R.K. Deka. Hall effects on MHD flow past an accelerated plate, Theoret. Appl. Mech. 35(4) (2008):333-346.

[5]. S.K. Ghosh, O.A. Beg, and M. Narahari. Hall effects on MHD flow in a rotating system with heat transfer characteristics, Meccanica 44 (2009):741-765. [

[6]. D.V. Krishna, D.R.V. Prasada Rao and A.S. Ramachandra Murthy. Hydromagnetic convection flow through a porous medium in a rotating channel, J. of Engng. Phys. And Thermophysics 75(2) (2002):281-291.

[7]. D.S. Chauhan and R. Agrawal. Effects of Hall current on MHD flow in a rotating channel partially filled with a porous medium, Chemical Engineering Communications 197(6) (2010):830-845.

[8]. D.S. Chauhan and R. Agrawal. Effects of Hall current on MHD Couette flow in a channel partially filled with a porous medium in a rotating system, Meccanica 47(2012):405-421.

[9]. Dileep Singh Chauhan, Priyanka Rastogi, Hall Effects on MHD Slip Flow and Heat Transfer Through a Porous Medium over an Accelerated Plate in a Rotating System, International Journal of Nonlinear Science, 14(2) (2012): 228-236.

[10]. M.VeeraKrishna and J.Prakash, Hall Current Effects on Unsteady MHD Flow in a Rotating Parallel Plate Channel Bounded by Porous Bed on the Lower Half—Darcy Lapwood Model, Open Journal of Fluid Dynamics, 5 (2015):275-294.

[11]. Ashaf A. Moniem, W.S.Hassanin, Solution of MHD flow past a vertical porous plate through a porous medium under oscillatory suction, Applied Mathematics, 4, (2013), 694-702.

[12]. B.Lakshmanna; S.Venkateswarlu, Heat and Mass Transfer on MHD Flow of an incompressible fluid past an infinite vertical porous plate", Journal of Ultra Scientist of Physical Sciences, Volume 29, Issue 9, Page number 234-247,2017.

[13]. M.Veera Krishna, M.Gangadhar Reddy, MHD Free Convective Boundary Layer Flow through Porous medium Past a Moving Vertical Plate with Heat Source and Chemical Reaction,Materials Today: Proceedings, vol. 5, pp.91–98, 2018. https://doi.org/10.1016/j.matpr.2017.11.058.

[14]. M.Veera Krishna, G.Subba Reddy, MHD Forced Convective flow of Non-Newtonian fluid through Stumpy Permeable Porous medium, Materials Today: Proceedings, vol. 5, pp. 175–183, 2018. https://doi.org/10.1016/j.matpr.2017.11.069.

[15]. M.Veera Krishna, Kamboji Jyothi, Hall effects on MHD Rotating flow of a Visco-elastic Fluid through a Porous medium Over an Infinite Oscillating Porous Plate with Heat source and Chemical reaction, Materials Today: Proceedings, vol. 5, pp. 367–380, 2018. https://doi.org/10.1016/j.matpr.2017.11.094.

[16]. B. Siva Kumar Reddy, M. Veera Krishna , K.V.S.N. Rao, R. Bhuvana Vijaya, HAM Solutions on MHD flow of nano-fluid through saturated porous medium with Hall effects, Materials Today: Proceedings, vol. 5, pp. 120–131, 2018. https://doi.org/10.1016/j.matpr.2017.11.062.

[17]. VeeraKrishna.M and B.V.Swarnalathamma, Convective Heat and Mass Transfer on MHD Peristaltic Flow of Williamson Fluid with the Effect of Inclined Magnetic Field," AIP Conference Proceedings, vol. 1728, p. 020461, 2016. DOI: 10.1063/1.4946512.

[18]. Swarnalathamma. B. V. and M. Veera Krishna, Peristaltic hemodynamic flow of couple stress fluid through a porous medium under the influence of magnetic field with slip effect AIP Conference Proceedings, vol. 1728, p. 020603, 2016. DOI: 10.1063/1.4946654.

[19]. VeeraKrishna.M and M.Gangadhar Reddy MHD free convective rotating flow of Visco-elastic fluid past an infinite vertical oscillating porous plate with chemical reaction, IOP Conf. Series: Materials Science and Engineering, vol. 149, p. 012217, 2016 DOI: 10.1088/1757-899X/149/1/012217.

[20]. VeeraKrishna. M and G.Subba Reddy Unsteady MHD convective flow of Second grade fluid through a porous medium in a Rotating parallel plate channel with temperature dependent source, IOP Conf. Series: Materials Science and Engineering, vol. 149, p. 012216, 2016. DOI: 10.1088/1757-899X/149/1/012216.

[21]. Veera Krishna.M., B.V.Swarnalathamma and J. Prakash, "Heat and mass transfer on unsteady MHD Oscillatory flow of blood through porous arteriole, Applications of Fluid Dynamics, Lecture Notes in Mechanical Engineering, vol. XXII, pp. 207-224, 2018. Doi: 10.1007/978-981-10-5329-0_14.

[22]. M.Veera Krishna, G.Subba Reddy, A.J.Chamkha, "Hall effects on unsteady MHD oscillatory free convective flow of second grade fluid through porous medium between two vertical plates," Physics of Fluids, vol. 30, 023106 (2018); doi: 10.1063/1.5010863.

[23]. Veera Krishna, M., Chamkha, A.J., Hall and ion slip effects on MHD rotating boundary layer flow of nanofluid past an infinite vertical plate embedded in a porous medium, Results in Physics, 15, 102652, DOI: https://doi.org/10.1016/j.rinp.2019.102652

[24]. Veera Krishna, M., Swarnalathamma, B.V., Chamkha, A.J., Investigations of Soret, Joule and Hall effects on MHD rotating mixed convective flow past an infinite vertical porous plate, Journal of Ocean Engineering and Science, 4(3), pp. 263-275, 2019. DOI: https://doi.org/10.1016/j.joes.2019.05.002.

[25]. Veera Krishna.M, Ali J. Chamkha, Hall effects on MHD Squeezing flow of a water based nano fluid between two parallel disks, *Journal of porous media*, 22(2), pp. 209-223, 2019. **DOI:** https://doi.org/10.1615/JPorMedia.2018028721